Process Window Enhancement for Single Point Incremental Forming through Multi-Step Toolpaths

J.R. Duflou (1) [1], J. Verbert[1], B. Belkassem[2], J. Gu[2], H. Sol[2], C. Henrard[3], A.M Habraken[3]
[1]Katholieke Universiteit Leuven, Department of Mechanical Engineering
[2]Vrije Universiteit Brussel, Department of Mechanics of Materials and Constructions
[3] Université de Liège, Department of Mechanics of Solids and Materials

Abstract
Single point incremental forming suffers from process window limitations which are strongly determined by the maximum achievable forming angle. Forming consecutive, intermediate shapes can contribute to a significantly enlarged process window by allowing steeper maximum wall angles for a range of part geometries. In this paper an experimentally explored multi-step toolpath strategy is reported and the resulting part geometries compared to simulation output. Sheet thicknesses and strains achieved with these multi-step toolpaths were verified and contribute to better understanding of the material relocation mechanism underlying the enlarged process window.

Keywords:
Incremental forming, Simulation, Multi-step toolpath

1 INTRODUCTION

Single Point Incremental Forming (SPIF) is a sheet metal part production technique in which sheet metal is formed in a stepwise fashion by a CNC controlled spherical tool. The flexibility of the process is mainly related to the fact that SPIF, in contrast with other forming processes, does not require a dedicated (partial) die to operate. As a result, the lead-time and cost of tooling can be avoided. This technique allows a relatively fast and cheap production of small series of sheet metal parts [1][2].

In addition to the achievable accuracy [3], one of the main drawbacks of the incremental forming process is the process limits. For every material with a given thickness a maximum forming angle α (see Figure 1) can be determined by means of a simple cone forming test as described in [1]. Secondary process parameters influencing the maximum forming angle, such as the tool diameter and incremental step size [4], are kept constant in this test. If a sufficiently large portion of a workpiece has a wall angle that exceeds this maximum angle, the part will fail during processing when using conventional toolpaths as described in [1].

In Table 1 a set of maximum wall angles for commonly used materials is given as a function of the thickness of the sheet and the diameter of the tool used during forming. These maximum wall angles limit the applicability of the process. Parts with (semi-) vertical walls are, for example, impossible to form using standard, straightforward milling toolpaths.

Material	Thickness (mm)	Tool Ø (mm)	Max. wall angle
Al 3003-O	1.2	10	71°
Al 3003-O	2.0	10	76°
AA 3103	0.85	10	71°
AA 3103	1.5	10	75°
Ti Grade 2	0.5	10	47°
DC01	1.0	10	67°
AISI 304	0.4	10	63°

Table 1: Common materials with their failure angles

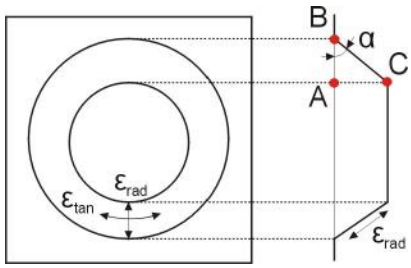

Figure 1: Top and sectional view of a cone

2 THEORETICAL BACKGROUND AND OBJECTIVE

The process limits of SPIF can be explained intuitively by the sine law. The zone of material AB in the original flat sheet (see Figure 1) will be stretched into the zone CB of the final part during the forming process.

$$T_{CB} = T_{AB} \sin(90 - \alpha)$$

Formula 1: Sine law

Assuming that only in-plane strains occur, the sine law can be used to estimate the final thickness of the part at zone CB (T_{CB}) from the original thickness of the zone AB (T_{AB}) and the wall angle of the part (α). It has experimentally been verified that the process follows this law [5] with a tendency to overform slightly [6].

From this formula it follows that the steeper the wall angle, the greater the thinning of the zone CB, with a wall angle of 90° resulting in a theoretical residual thickness (T_{CB}) of zero. In order to increase the maximum wall angle, one could increase the starting thickness (T_{AB}) of the sheet, as can be seen in the experiments reported in Table 1. This strategy has its limitations due to maximum machine load and overall part thickness specifications. The diameter of the tool and the selected stepdown also have a limited impact on the maximum forming angle [4]. Finally, the only way to obtain large wall angles is to aim for material redistribution by shifting material from other zones in the part to the inclined wall areas. Several authors have already reported on multi-pass forming. Consecutive toolpaths, corresponding to virtual parts with increasing wall angles, are being executed in a multi-step procedure. Typically a large offset from the backing plate is favoured for the first passes since this allows for more

bending, avoiding extreme strains near the top of the part [6][7][8].

The aim of this paper is to further investigate the mechanics behind the multi-step forming approach to contribute to a better understanding of the material relocation mechanism underlying the enlarged process window.

3 EXPERIMENTAL EXPLORATION

3.1 Experimental Setup

The experiments were performed on a three-axis milling machine with a horizontal spindle. This allowed in-process observation of the part being formed by means of a stereo camera setup and Digital Image Correlation (DIC).

For each of the tests, a spherical tool with a diameter of 10mm was chosen with the feedrate set to 2m/min and the spindle speed fixed at 100 rotations/min. Oil was used as lubricant. The setup allowed to remove the part within its clamping rig from the machine, without unclamping the part itself. This allowed the part to remain clamped during consecutive manufacturing and measuring steps.

To obtain the thickness and accuracy profiles, the part was removed from the milling machine and scanned with a laser line scanner with an accuracy of ±15µm, mounted on a CMM machine. This yielded a point cloud of about 0.4 million measurement points per scanned part, which were further processed into the profiles presented in this paper.

3.2 Comparison of the thickness distribution for single and multi-step formed parts

For the first set of experiments, two cones of 70 degree wall angle were manufactured. Both cones have an upper inner diameter of 178mm and a programmed internal depth of 30mm. The diameter of the backing plate was 182mm, close to the part to eliminate most of the bending that is induced by multi-step forming. A single-step reference part was compared with a part formed with two intermediate steps at 50° and 60°. The sheet material used for these tests was Al3003-O with a thickness of 1.2mm.

In Figure 2 the thickness profiles of both cones are plotted in function of the depth. The theoretical sine law thickness for a 70° cone is plotted as well. As can be seen, the wall thickness of the multi-step cone is significantly larger than the thickness obtained with the single-step toolpath. However, the thickness of the bottom of the multi-step part is lower than the thickness of the bottom of the single-step part. This can be seen more clearly in Figure 3 where the thickness is plotted against the part radius. Using the multi-step approach has clearly led to a shift of material from the bottom, which would otherwise have remained unprocessed, to the wall of the part. Side effect is that the bottom of the part is no longer flat but slightly curved and deeper than the programmed CAD file (see Figure 2).

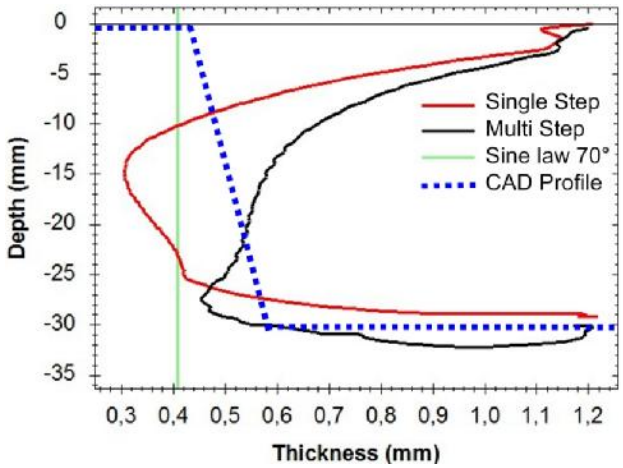

Figure 2: Thickness in function of depth

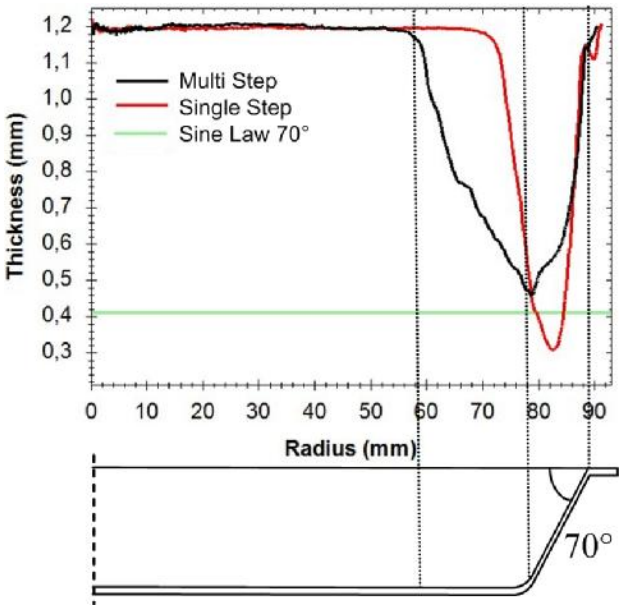

Figure 3: Test part geometry and thickness in function of radial dimension

3.3 Forming of a cylindrical part in 5 steps

Test setup

Aim of this experiment was to quantify the material flow during multiple consecutive steps of forming. A cylindrical wall was manufactured in 5 passes with a 10° increase in the wall angle between each step, starting from 50°. The intermediate shapes were chosen in order to eliminate folding over between successive steps. If the angle increment between two consecutive steps is too large, the horizontal distance between two steps at a certain depth will become too big compared to the tool diameter, and folding over, resulting in failure, will occur. The angle increase between steps, and consequently the number of intermediate shapes required, is therefore dependant on the desired height of the 90° wall one wants to create and the diameter of the tool used. The deeper the part, the more steps will be required to eliminate folding.

The sheet material used for these tests was AA3103 with a thickness of 1.5mm. The workpiece had an upper diameter of 128mm and a programmed depth of 30mm. The diameter of the backing plate was 131mm, close to the part to eliminate most of the bending that is induced by multi-step forming. A 10mm diameter tool and a contouring toolpath were used with a stepdown of 1mm per contour.

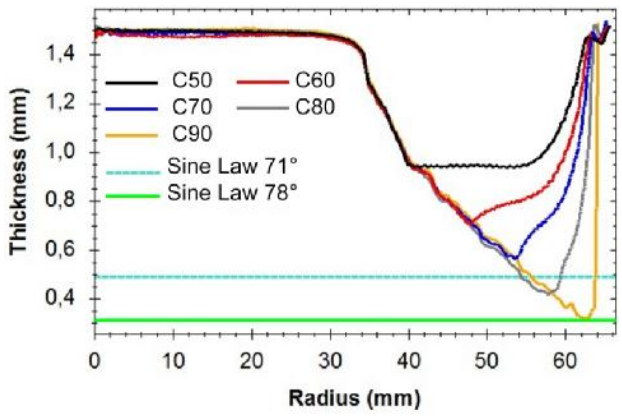

Figure 4: Thickness in function of radial dimension

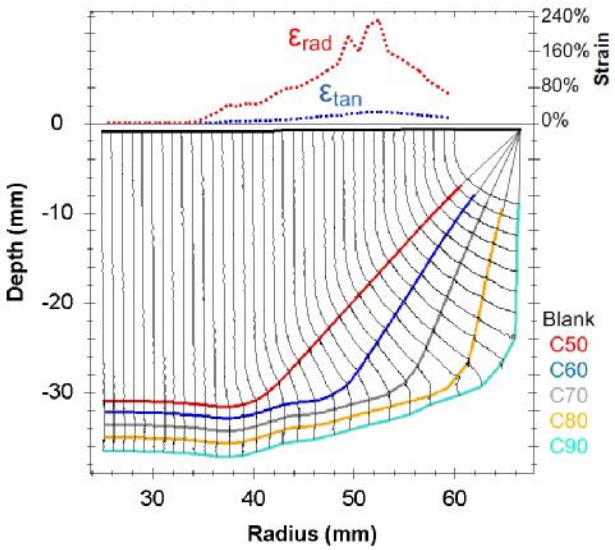

Figure 5: Measured outer surface evolution and final strain distribution

Experimental results

In Figure 4 the thickness profiles of the cones in the different steps and the theoretical sine law thickness are plotted against the radial dimension. The bottom of the part (0 to 32mm radius) was unprocessed and is still at nominal thickness (1.5mm). As can be seen, the thickness profile of the first step (C50) determines the thickness profiles of the following steps. The part was close to failure near the bottom since the thickness of the 90° part is, at its thinnest point, lower than the failure thickness as predicted by the sine law for 71°. In fact the thickness of the 90° part corresponds to a sine law thickness for a 78° cone, meaning that the wall of the cone has been thinned well below the normal failure limit corresponding to a 1.5mm sheet thickness (see Table 1).

In Figure 5 the experimentally measured evolution of the profiles of the cones is plotted. 36 points, defining a planar section of the outer surface of the cone, were tracked during the forming process by means of a Limess stereo camera setup and DIC. The coloured curves represent the shape of the part at the end of each of the five consecutive forming steps. The black curves visualise the trajectories of each of the observed points on the outer part surface based on 2030 intermediate observations.

Tangential strains, ε_{tan} as defined in Figure 1, were calculated based on the radial locations, taking into account the axis-symmetrical nature of the workpiece. The thickness corresponding to the radial and tangential strains was calculated as well and, taking into account the accuracy of the used measurement systems, corresponds well with the thickness measurements obtained by laser scanning (Figure 6).

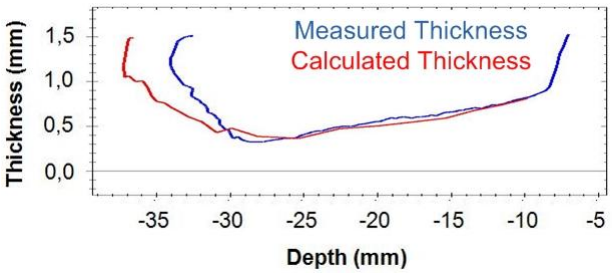

Figure 6: Measured and calculated thickness profiles

As can be seen in Figure 5, the sine law is an acceptable approximation for the first step of the multi step approach: when forming the first, 50° cone, the points are translated quasi downwards. This corresponds to a very limited tangential strain. For the next steps, however, the sine law is no longer valid. Instead of a downward translation, the points are quasi rotated about the backing plate edge, which causes a more substantial tangential strain that increases towards the bottom of the part (up to 25%: see Figure 5). The closer to the bottom of the part, the larger the horizontal distance between two consecutive step sections becomes and the more the rotational motion transforms into a downward translation. The maximum strains in both radial and tangential directions occur at the lower wall edge in the final stage of the vertical wall forming. In contrast with single-step forming, where maximum thinning and failure typically occur 10 to 15mm below the backing plate level when forming a cone, the edge of the cone bottom is also the location where failure can be expected to occur first in a multi-step strategy.

4 FEM SIMULATION

In this section, the simulation and experimental validation of the manufacturing of a cylindrical part were compared. The workpiece used in these tests has an upper inner diameter of 178mm and a programmed inner depth of 30mm. The part was formed in 5 steps with a 10° increase in wall angle between each step, starting from 50°. The sheet material used for these tests was Al3003-O with a thickness of 1.2mm.

Model Description

The simulations were performed using Lagamine, a finite element code developed at the University of Liège [9]. The implicit time integration scheme was chosen here in combination with a second order shell element called COQJ4 [10]. This model was found to provide the best compromise between accuracy and computation time.

In order to limit the computation time, the test part was modelled as a 45-degree segment with symmetry imposing boundary conditions at the edges. Even though the process itself is not rotationally symmetric, this approximation was found to provide useful results in the middle of the pie segment, i.e. sufficiently far from the model boundaries. The mesh contained 2320 elements.

The material model used was a Hill law with Swift-type isotropic hardening, for which the parameters were determined by means of a tensile and a Bauschinger shear test.

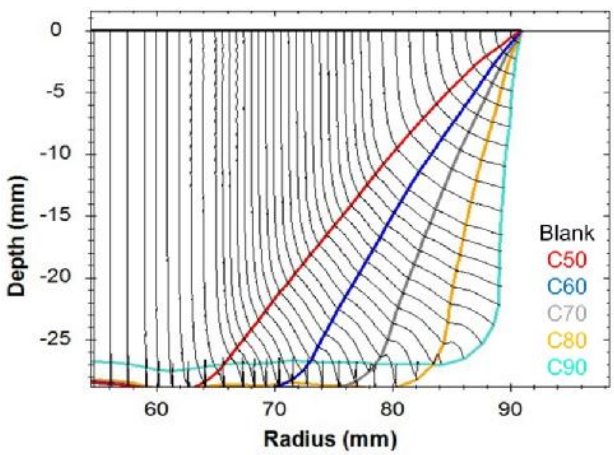

Figure 7: Simulated outer surface evolution results

Figure 7 illustrates that the bottom of the workpiece is not as accurately predicted as the wall. The symmetry imposing boundary conditions introduce an error. It has already been shown in a previous article [11] that the bottom of a single-step cone could be predicted more accurately if the whole part was modelled. This deviation seems to accumulate when simulating a multi-step toolpath. The obtained wall geometry and the simulated strains however correspond well with the experimentally obtained results.

The simulation stopped two contours before the end of the simulation. Therefore the blue curve in Figure 7, which represents the measured profile of the 90° part, is higher than the previous curves. This is due to the large deformation that some elements underwent at that stage of the process. A complete simulation would require remeshing after the third or fourth step. This remeshing is under development in the Lagamine code and will be reported in future publications.

5 CASE STUDIES

A method for automatic multi-step toolpath generation was developed and successfully tested in a number of case studies.

The part in Figure 8, a mould for composite pressure vessel production, has a vertical wall of 30 mm on top of which a hemisphere is modelled. For the material used (AA3103) and a 1.5 mm sheet thickness, this leads to a geometry which exhibits wall angles above the conventional process limits for the first 60 mm of the part.

Figure 9 illustrates that also for non-rotative geometries the multi-step approach remains applicable. The limits for achievable minimum radii between vertical walls are object of further research. Figure 10 depicts a skull implant manufactured in 0.7 mm grade 2 titanium. A multi-step toolpath made it possible to form wall angles up to 61° while respecting the minimum thickness requirements.

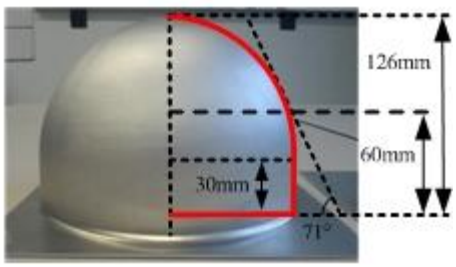

Figure 8: Composite pressure vessel mould

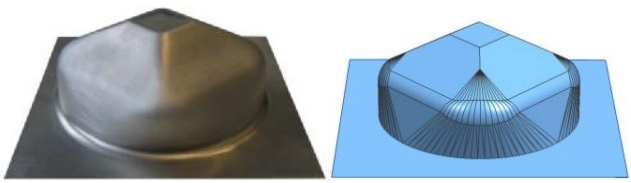

Figure 9: Non-rotational part

Figure 10: Titanium cranial implant
(right image courtesy of SimiCure)

6 CONCLUSIONS

The extended process window achievable by means of multi-step SPIF can be explained by the straining of (semi-) horizontal workpiece areas that remain unaffected in conventional toolpath strategies. This allows to produce vertical walls without leading to part failure. While a significant decrease in radial strains can be observed in steep walls compared to single-step forming, the multi-step toolpath strategy results in substantial tangential strains. The resulting thinning of the sheet during multi-step forming can exceed the maximum thickness reductions observed in single-step processing, implying a formability shift. Failure criteria based on detailed strain history analysis are part of ongoing research.

By means of a number of case studies the applicability of multi-step toolpath strategies for forming part geometries exceeding conventional single-step forming limits was demonstrated. From these case studies it can be concluded that there is no reason to consider 90° wall angles as the ultimate process limit. This opens perspecitves for further experimental exploration.

7 REFERENCES

[1] Jeswiet J., Micari F., Hirt G., Bramley A., Duflou J.R. and Allwood J., 2005, Asymmetric single point incremental forming of sheet metal. CIRP Annals - Manufacturing Technology, 54/2:623-649

[2] Matsubara S., 1994, Incremental backwards bulging of sheet metal with an hemispherical head tool, J.Japan Society for Techn. of Plasticity 5:119-123

[3] Duflou J.R., Lauwers B., Verbert J., Tunckol Y., De Baerdemaeker H., 2005, Achievable Accuracy in Single Point Incremental Forming: Case Studies, Proc. of the 8th Esaform Conf. Vol. 2., pp. 675-678.

[4] Ham M., Jeswiet J., 2007, Forming Limit Curves in Single Point Incremental Forming, CIRP Annals-Manufacturing. Technology, 56/1:277-280.

[5] Matsubara S, 2001, A computer numerically controlled dieless incremental forming of a sheet metal, Journal of Engineering Manufacture. 215/7:959–966

[6] Young D. and Jeswiet J., 2004, Wall thickness variations in single-point incremental forming, Journal of Engineering Manufacture, 18/11:1453-1459

[7] Kim T.J., Yang D.Y., 2001, Improvement of formability for the incremental sheet metal forming process. Int. J. of Mech. Sciences, 42:1271-1286

[8] Hirt G., Ames J., Bambach M, and Kopp R. , 2003, Forming strategies and Process Modelling for CNC Incremental Sheet Forming, CIRP Annals - Manufacturing Technology, V53/1, pp 203-206

[9] Cescotto S. and Grober H., 1985, Calibration and Application of an Elastic-Visco-Plastic Constitutive Equation for Steels in Hot-Rolling conditions, Engineering Computations, 2:101–106

[10] Jetteur P. and Cescotto S., 1991, A Mixed Finite Element for the Analysis of Large Inelastic Strains, International Journal for Numerical Methods in Engineering, 31:229–239

[11] He S., Van Bael A., Van Houtte P., Szekeres A., Duflou J.R., Henrard C. and Habraken A.M., 2005 Finite Element Modeling of Incremental Forming of Aluminum Sheets, Advanced Materials Research, Vol. 6-8:525–532